A rheological approach to assess the printability of thermosensitive chitosan-based biomaterial inks

To cite this article before publication: Maedeh Rahimnejad *et al* 2020 *Biomed. Mater.* in press https://doi.org/10.1088/1748-605X/abb2d8

IOP Publishing Biomedical materials
https://doi.org/XXXX/XXXX

A Rheological Approach to Assess the Printability of Thermosensitive Chitosan-based Biomaterial Inks

Maedeh Rahimnejad[1a], Thierry Labonté-Dupuis[2a], Nicole R. Demarquette[2] and Sophie Lerouge[1,2a*]

[1]Biomedical Engineering Institute, School of Medicine, Université de Montréal, Canada
[2]Department of Mechanical Engineering, École de technologie supérieure (ÉTS), Canada
[a]Research Centre, Centre Hospitalier de l'Université de Montréal (CRCHUM), Canada
[*]Corresponding author
E-mail: sophie.lerouge@etsmtl.ca

Abstract

For extrusion-based bioprinting, the inks must be printable and rapidly present sufficient mechanical properties to support additional layers and provide a cohesive, manipulable structure. Thermosensitive hydrogels may therefore be interesting candidates. However, the use of these materials is particularly challenging since their rheological properties evolve with time and temperature. In this work, a rheological approach to characterize the printability of chitosan-based thermosensitive inks was developed. The method consists of evaluating:1) the gelation kinetic at room temperature and at 37C; 2) shear thinning behavior to estimate the shear rate applied during printing as a function of printing parameters; 3) the viscosity after shear removal (recovery test) to simulate behaviour after biomaterial deposition. Hydrogels containing 2 and 3%w/vol chitosan, combined with different gelling agents (Sodium-hydrogen-carbonate (SHC), Phosphate-buffer, Beta-glycerophosphate (BGP)) were tested, and compared with alginate/Gelatin bioink as controls. To correlate the rheological studies with real printing conditions, 3D-Discovery bioprinter was used to print hydrogels and the visual aspect of the printed structure was observed. Unconfined compressive tests were carried out to study the impact of applied shear rate during printing on the mechanical properties of printed structures. All pre-hydrogel solutions presented shear thinning properties. The recovery of viscosity was found to depend on the hydrogel formulation, as well as the level of shear rate and the state of gelation at the time of printing. Formulations made with SHC and phosphate buffer presented too rapid gelation and phase separation,leading to poor printing results. One particularly promising formulation composed of SHC and BGP, when printed at a shear rate of $140s^{-1}$, before its gelation time ($t_g \leq 15$min), resulted in good printability and 3D structures with rigidity comparable with the Alginate/Gelatin bioink. The methodology introduced in this paper could be used to evaluate the printability of other time- and temperature dependent biomaterial inks in the future.

Keywords: biomaterial inks, chitosan thermosensitive hydrogel, printability, extrusion-based bioprinting, rheology

1. Introduction

Among the various challenges of extrusion-based bioprinting, one is to design biomaterial inks and bioinks that fulfill the numerous requirements. The ink must be extrudable e.g. injectable through a small needle to reach high resolution but rapidly possess sufficient mechanical properties to keep the structure intact, support additional layers and provide a cohesive, manipulable structure [1]. Moreover, for bioinks, the material and the printing process must be cell friendly [2, 3]. It should ideally also be biodegradable to be gradually replaced by extracellular matrix. All these requirements explain why the search for ideal biomaterials is still ongoing. Moreover, standard methods to characterize and optimize biomaterial inks and bioinks have yet to be developed [4-7].

Among the biomaterials that could be used for bioprinting, chitosan-based hydrogels are attractive candidates due to their biocompatibility, biodegradability, low cost and thermosensitive properties. Chitosan, a natural biopolymer derived from chitin, can be dissolved in acidic solution. When combined with a weak base such as beta-glycerophosphate (BGP), it can form a solution with physiological pH that rapidly gels with increasing temperature [8-10]. However, the mechanical properties of such gel are quite poor. Our team showed that using new combinations of gelling agents (namely a mixture of sodium hydrogen carbonate (SHC) with

phosphate buffer (PB) or BGP), we can strongly enhance the mechanical properties of the hydrogels, while ensuring physiological osmolality and rapid gelation at 37°C [11, 12]. These gels allow excellent cell survival and growth and were demonstrated as very interesting candidates for injectable cell-loaded scaffolds for cell therapy and tissue engineering [12, 13].

Chitosan thermosensitive properties also make them potential candidates for bioprinting, as the gel is in the form of a viscous solution at room temperature prior to its gelation through increasing temperature, which can be achieved using a warm substrate or incubator. Rapid physical crosslinking can help to keep the post-printed structure mechanically intact and prevent hydrogel dispersion, without the addition of a crosslinker or photopolymerization step; A few teams have already shown the potential of such thermosensitive hydrogels for bioprinting, alone or mixed with gelatin or hydroxyapatite [14, 15]. However, the use of these materials for bioprinting is particularly challenging since their rheological properties evolve with time and temperature. While most teams perform temperature ramps and time sweep to follow the gelation kinetics at body temperature, there has been to date no complete rheological study to characterize and optimize their printability. More generally, there is presently a lack of appropriate methods to study the printability of time- and temperature evolving materials like those.

The general aim of the present work is to propose a rheological approach to study the printability of thermosensitive hydrogels, which takes into account the time and temperature-induced gelation process. We then used this methodology to assess the potential of the chitosan thermosensitive hydrogels as biomaterial inks, in comparison with alginate/gelatin bioink which has been already demonstrated for its excellent printability [6].

In order to be used in extrusion-based deposition process a biomaterial ink must present a viscosity that allows its extrusion. It also must present shear recovery (rapid recovery of the initial viscosity once shear has stopped). An important parameter to calculate is therefore the shear rate applied during extrusion. During extrusion, the ink flows through a capillary and is subjected to a shear rate ($\dot{\gamma}_W$) given by equation 1 [16]:

$$\dot{\gamma}_W = \frac{4Q}{\pi R^3}\frac{3n+1}{4n} \quad \textbf{(1)}$$

Where Q (mm^3s^{-1}) is the flow rate; R (mm) is the inner radius of the needle; and (n-1) is the slope of the viscosity versus shear rate graph on a log log plot.

Indeed, most materials are shear thinning, i.e., their viscosity decreases with increasing shear rate. Therefore, to evaluate the shear rate a bioink undergoes during bioprinting, it is first necessary to measure the viscosity as a function of shear rate [17-19]. However, carrying out rheological characterization of hydrogels can be difficult when their rheological properties are time-dependent. A simple shear rate ramp (viscosity as a function of varying shear rate) [16] is not appropriate. In those cases, since the viscosity also changes with time, the tests must be adapted in consequence.

Once a layer is printed, it needs to rapidly reach enough mechanical properties to support gravity and keep its form as well as to support other layers. In some cases, such as alginate-based bioinks, ionic crosslinking can be performed by immersion in a calcium ion rich solution after printing. Other materials can be photopolymerized layer by layer. In the case of thermosensitive hydrogels such as chitosan, rapid shear recovery is particularly important since no rapid crosslinking method can be applied between layers.

These characteristics can be evaluated using rheological tests, consisting of evaluating the biomaterial ink viscosity as a function of time once the shear rate encountered by the ink during extrusion has been applied and removed. This test is called the recovery test [19]. Performing recovery tests at different shear rates allows to estimate the maximum shear rate that should be applied during printing, i.e. at which the hydrogels return rapidly to their primary viscosity after shear removal without breakage. A potential advantage of thermosensitive hydrogels is that after printing the hydrogel continues to gel at 37°C. The recovery test must therefore be adapted to take this behaviour into account.

The hydrogel gelation kinetic is also an important parameter that determines the suitability of the hydrogel for extrusion-based bioprinting [20]. Indeed, whether gelation has been initiated at the time of printing probably has an impact on recovery after shear removal, uniformity and resolution, as well as mechanical properties. The gelation kinetics of chitosan hydrogels therefore need to be assessed at various temperatures reproducing the steps of the bioprinting process, in particular at room (storage in the cartridge and extrusion) and body temperature (substrate warming or incubator).

In this work, we show how this rheological approach can be applied to assess the printability and the time frame optimal

for bioprinting thermosensitive hydrogel. In particular, we apply this approach on chitosan hydrogels of various composition, in terms of chitosan concentration and the type and concentration of gelling agents. Post-printed resolution, integrity and mechanical properties were also characterized and compared with values obtained for a previously published bioink composed of alginate and gelatin [21].

2. Materials and methodology

2.1 Materials

Shrimp shell chitosan (ChitoClear, HQG110, Mw: 155 kDa, DDA 83%) was purchased from Primex (Iceland). β-Glycerol phosphate disodium salt pentahydrate ($C_3H_7Na_2O_6P{\cdot}5H_2O$, hereafter BGP), sodium phosphate monobasic NaH_2PO_4 (SPM) and sodium phosphate dibasic Na_2HPO_4 (SPD) were purchased from Sigma-Aldrich (Oakville, ON, Canada). Sodium hydrogen carbonate $NaHCO_3$ (sodium bicarbonate, hereafter SHC) was purchased from MP Biomedicals (Solon, OH, USA). Sodium alginate salt from brown algae, Type B gelatin from bovine skin (G9391) and calcium chloride ($CaCl_2$) were purchased from Sigma-Aldrich. Other chemicals were of reagent grade, and were used without further purification.

2.2 Preparation of chitosan thermosensitive hydrogels

2.2.1 Chitosan solution

Chitosan powder was solubilized in hydrochloric acid (HCl) (0.09 M and 0.013M) at 3.33% w/v (for final concentration 2%) or 5%w/v chitosan (final 3%), respectively, with mechanical stirring for 2 hours. The solution was sterilized by autoclaving (20 min, 121°C) and stored at 4°C.

2.2.2 Gelling agent (GA) solutions

Three different GAs were used in this study, namely BGP, SHC, and PB at pH = 8. PB was prepared with a mixture of sodium phosphate dibasic and sodium phosphate monobasic at ratio of ratios of 0.047/0.540 w/w in milli-Q water. SHC was combined with either PB or BGP as previously published [11].

2.3 Preparation of pre-hydrogel solutions for rheological characterization

Chitosan pre-hydrogel solutions were prepared by mixing CH solution with one of the GA solutions at a volume ratio of 3:2, respectively. The two solutions were introduced in separate syringes, joined by a Luer lock connector. The content of the GA syringe was pushed into the CH syringe and the mixture was pushed from side to side for 15 repeats immediately prior to use. Pre-hydrogel solutions were then centrifuged to remove air bubbles and used immediately. Table 1 summarizes all formulations tested. Hydrogels formed with a mixture of SHC and BGP as gelling agents are identified as A, and those formed with SHC and PB as B. Hydrogels had a final chitosan concentration of 2% (w/v) or 3% (w/v). All had a physiological pH.

Table 1: Concentration of chitosan and gelling agents of the various tested hydrogels (CH: Chitosan, BGP: Beta-glycerophosphate, SHC: Sodium hydrogen carbonate, PB: Phosphate buffer at pH=8).

Hydrogel name	**[GA component] (M)**			**Final concentration of CH% (w/v)**
	SHC	**BGP**	**PB**	
A2	0.075	0.10	-	2
A3	0.113	0.15	-	3
B2	0.075	-	0.02	2
B3	0.113	-	0.03	3

2.4 Preparation of alginate/gelatin hydrogel (control group)

Sodium alginate and Type B gelatin powders were dissolved in milli-Q water, and stirred using a magnetic hotplate for 1 hour at 60°C and 2 hours at room temperature to achieve a homogeneous composite precursor comprised of 3 w/v% alginate and 7 w/v% gelatin as explained in detail by Kinsella's group [21]. The Alginate/Gelatin solution was then kept 2 hours at room temperature to remove air bubbles and later stored at 4°C. Before use, the solution was warmed at 22°C for 30 min [21] and centrifuged to remove air bubbles. A 1%w/v $CaCl_2$ solution for crosslinking the alginate was also prepared by dissolving $CaCl_2$ into milli-Q water.

2.5 Rheological tests

Rheological properties were carried out using an Anton Paar instrument (Physica MCR 301, Germany) with a cylinder geometry (CC10/T200), (1mm gap) or plate-plate geometry (PP25) of 25 mm diameter. Linear viscoelastic (LVE) range was first determined through amplitude sweep test using PP25. The following tests were then performed:

1) Time sweeps at 22 & 37 °C for 1 hour were performed using the oscillatory mode in the LVE range, at a constant shear strain (1%) and constant frequency (1Hz). They allowed the study of gelation kinetic at both temperatures, as a function of gel composition, by following values of complex viscosity, the storage and loss modulus (G' and G'') and loss factor tan $\delta = G''/G'$ as a function of time.

2) Viscosity behavior of the pre-hydrogel solutions at 22°C was assessed using rotational rheometry tests. In contrast to conventional shear thinning tests, where the viscosity change is reported with varying shear rate, here the viscosity was studied as a function of time at different shear rates (0.01, 0.1, 1, 10, 100 s^{-1}). This was done to take into account the possible variation of pre-hydrogel properties with time. To express the shear thinning behavior, the viscosity values at one particular time point were then plotted as a function of shear rate. A time point of 10 min was chosen assuming this corresponds to the time required for hydrogel preparation and printing (including mixing of chitosan solution and gelling agent, centrifugation of the solution and loading on the print head).

3) Shear recovery after different levels of shear rate (low to high-10 to 1000 s^{-1}) was evaluated using rotational rheometry. The viscosity was measured during the consecutive steps which mimic the printing process: (1) Pre-printing (shear rate of 0.001 s^{-1} for 10 min at 22°C); (2) Printing (sudden increase of shear rate at 10, 100, 500 or 1000 s^{-1} for 1 min at 22°C); (3) Post printing (shear rate of 0.001 s^{-1} for 10 min at 22°C and then increasing the temperature to 37°C to take advantage of the hydrogel thermosensitivity) (Figure 1).

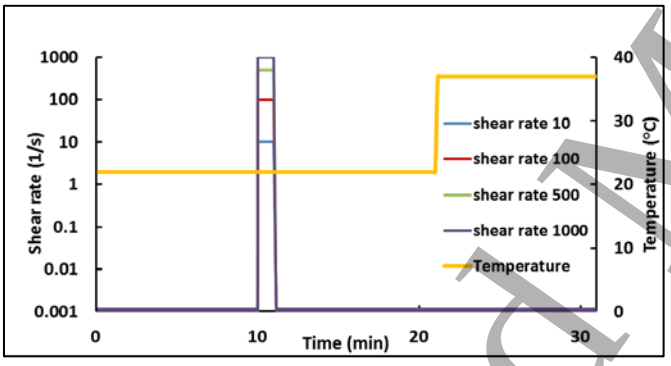

Figure 1. Schematic of the applied shear rates and temperature as a function of time during recovery tests.

2.6 Printing procedure

A 3D-Discovery (RegenHU) bioprinter was used to print the hydrogels via a plunger dispenser which enables to keep the dispensing rate constant during printing (volume/min) even if the hydrogel properties change with time. The cartridge was kept at room temperature, while the heated substrate temperature was kept constant at 37°C. Different steel needles (sizes 22G/25G, length: 0.25 inch) were used to print hydrogels. Printing parameters are presented in Table 2. The flow rate of the bioink, the layer thickness (h) and the translational speed of the printing head (feed rate) (V_t) were chosen to ensure that we have proper and continuous filament formation, and were kept constant throughout the study. The shear rate applied during printing was calculated according to Equation 1, using the slope of the viscosity versus shear rate graph (n-1) on a log log plot, and reported in Table 2.

2.7 Printing resolution, hydrogel uniformity and structural integrity

Each biomaterial ink formulation was printed using two different needle sizes (22G/25G) according to the conditions in Table 2. Images were taken from each print and analyzed using the freeware ImageJ (Fiji.sc) according to the approach studied by Gillispie et al. [22] and Webb et al. [23]. The average width of printed filaments was determined, for each printing setting, by manually selecting 6 random points. We also evaluated the quality of the angle printed (sharp (1) versus curvy (0)) and the continuity of the lines ((1) versus (0) if more than one break observed). The width of the line was also compared to the internal diameter of the needle (width/diameter). A high ratio means that the gel spreads a lot after printing, decreasing the printing resolution.

Table 2. Printing parameters used on the 3D Discovery bioprinter: needle size, n-1 slope according to viscosity vs shear rate graph and corresponding shear rate as a function of needle size according to equation 1. Constant parameters were: Flow rate = 1.25 µL/s (mm^3/s); feed rate = 6 mm/s; layer thickness = 0.3 mm.

Pre-hydrogel solutions	**Needle size**		**Slope of viscosity vs shear rate (see Equation 1) (n-1)**	**Shear rate (s^{-1})**
	Gauge	**Inner diameter (mm)**		
A2	22	0.41	-0.3	203
	25	0.25		897
A3	22	0.41	-0.5	230
	25	0.25		1017
B2	22	0.41	-0.6	250
	25	0.25		1101
B3	**Not printable (lack of homogeneity and continuity)**			

To assess structural integrity, the best printable formulation was printed in 10-layer and 20-layer honeycomb structures and the theoretical height (layer thickness multiplied by number of layers) was compared to real height after 1hour incubation at 37°C (to assure solidification).

2.8 Post-printed mechanical properties

Unconfined compression tests were performed on 5-layer printed honeycomb structures using the MACH-1 testing device (Biomomentum, Canada). A velocity equal to 100% of the sample's height/min was used. The compressive strength and the secant Young modulus at 15% and 30% of deformation were calculated from the stress-strain curves. ImageJ software was used to calculate the real surface area of the printed structure (without the holes in the structure) for measurement of applied stress. Mechanical properties were compared with those of structures fabricated with Alginate/Gelatin bioink. Tests were performed at room temperature after 24 hours of sample gelation at 37°C.

2.9 Statistical analyses

All experiments were performed at least in triplicate. Results were expressed as mean ± SD. Statistical analysis was performed using GraphPad Prism 7.04 software. One-way ANOVA and Tukey's multiple comparison tests were used to compare multiple groups. $P<0.05$ was considered to be statistically significant.

3. Results

3.1 Time sweep at 22 and 37°C

Time sweeps were performed in the LVE region, first at room temperature (22°C) to estimate the stability of the pre-hydrogel solutions in the printing cartridge as a function of their composition (Figure 2a) but also at 37°C to estimate their kinetic of gelation (solidification) once on the heated substrate (Figure 2b). Both figures present the evolution of the storage (G') and loss (G'') moduli. The viscous pre-hydrogel solution is considered to become a viscoelastic gel when G'>G''. According to the approach of Winter and Chambon [24], we considered the gelation time as the time where $G' = G''$, or the loss factor $\tan\delta=G''/G'=1$. Figure 2(c) summarizes the mean G' value after 10 min at 22°C (considered as the printing time) and after 1 hour at 37°C (to mimic 1 hour after printing). At 22 °C (Figure 2(a)), the gelation time is less than 15 s (G'>G'' already at the first measurement) and 30 s for B2 and B3 hydrogels respectively. For A2 and A3, it takes several minutes to begin gelation (t_{gel} = 5±3.4 and 15±7.5 min respectively). B formulations also show higher values of storage modulus compared to A formulations. As expected, A3 gel (CH3%) presents higher storage moduli right after preparation than its A2 counterpart (CH2%). In contrast, B2 and B3 show similar storage modulus as a function of time.

The evolution of the storage (G') and loss (G'') moduli at 37°C as a function of time is presented in Figure 2(b). Drastic increase of G' value during isotherms at 37°C is indicative of the gel thermosensitivity. Thermosensitivity is more evident with CH 2% formulations rather than 3%. While A2 and B2 present the lowest modulus at 22°C, they rapidly increase at 37°C, leading to the highest values after 1hour gelation, B2 being significantly higher than all others ($p<0.001$, Figure 2(c)). In contrast, A3 and B3 present higher initial viscosity (not shown here) and slowly gel at 37°C. Their properties after 1-hour gelation are relatively similar.

At printing time (after 10 min at 22°C), B3 formulation presents the highest storage modulus values ($p<0.0001$), while the difference among the three other formulations is not significant (Figure 2(c), left panel). As will be discussed later, this leads to difficult control of printing and reproducibility.

3.2 Shear thinning behavior

The shear thinning property of the solution is a critical property for bioprinting. Figure 3 presents the shear thinning behavior of A2 and A3 formulations. Results of B formulations and Alginate/Gelatin are shown in supporting information (Figure S2). As explained in the materials and methods section, since the viscosity is changing as a function of time, shear thinning properties were evaluated by measuring the viscosity over time at 5 different applied shear rates (from 0.01 to 100 s^{-1}). Figure 3(a) presents the 5 viscosity curves as a function of time for sample A3. Then, the values at one particular time point (here 10 min) were plotted to form the curve of viscosity versus shear (Figure 3(b)). Results showed that both chitosan A2 and A3 pre-hydrogel solutions present shear thinning properties, characterised by a sharp decrease in viscosity value with increasing shear rate, with some differences between the gel formulations. Shear thinning was also observed for B formulations, as well as for the alginate/ gelatin (control group), although to a lesser extent (viscosity decrease from 10000 to 100 Pa.s only) (Supplemental data_Figure S2).

Surprisingly, a variation of the viscosity as a function of time was seen only at the lowest shear rate (0.01 s^{-1}) (Figure 3(a)). Since the solutions are not completely stable at room temperature (as just shown), we were expecting the viscosity to increase with time at all shear rates. This suggests that shear rates equal or above 0.1 s^{-1} prevent the physical gelation of the chitosan bioinks, and demonstrates the importance of testing conditions on rheological results.

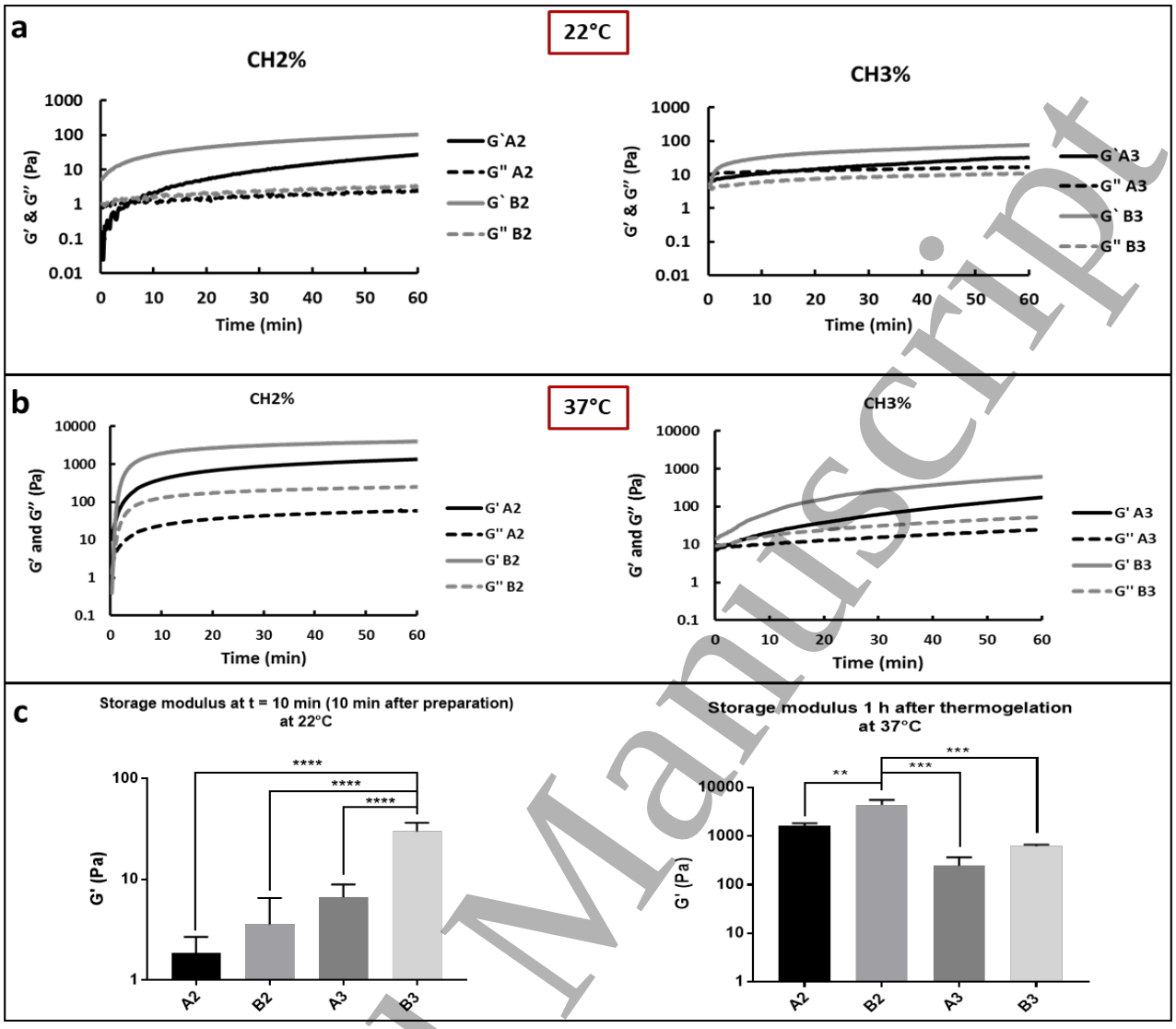

Figure 2. Gelation kinetics of A and B chitosan-based hydrogels: a) Evolution of the storage (G') and loss (G'') moduli of hydrogels as a function of time at 22°C (mean +/-SD; n≥3). b) Evolution of the storage (G') and loss (G'') moduli as a function of time at 37°C. c) G' value after 10 min at 22°C and 1h at 37°C, respectively (mean +/-SD; n≥3); (** p<0.01, *** p<0.001, **** p<0.0001). Gels were made with SHC+BGP as gelling agents, while B gels were prepared with SHC+PB, as described in Table 1.

We used the slope of the shear thinning test at shear rate between 10 and 100 s^{-1} to calculate the shear stress during printing using equation 1 as presented in the introduction and reported on Table 2.

3.3 Shear recovery

We concentrated on A formulations due to their slower gelation kinetics at room temperature and more homogenous fiber formation at extrusion (shown later in the manuscript). In accordance to the schematic presented in Figure 1, shear recovery tests followed the evolution of the viscosity during rest (shear rate = 0.001 s^{-1}), followed by applying shear for 1 min and let recover after shear removal at 22°C (to simulating the printing procedure), followed by temperature increase from 22 to 37°C. To study the influence of the extent of shear rate on recovery, four different applied shear rates were compared, from 10 to 1000 s^{-1}.

Figures 4(a) and (c) present the results for A2 and A3 formulations respectively. In accordance with the previous results, the viscosity increased with time at rest, followed by sudden drop during shear due to shear thinning. Viscosity

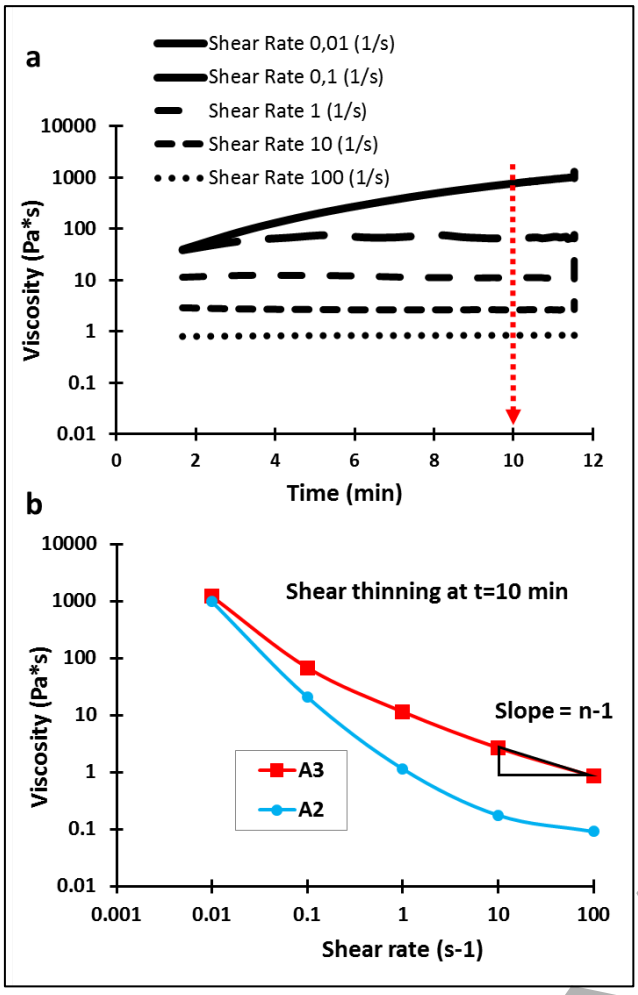

Figure 3. Shear thinning behavior of: a) viscosity of A3 formulations at various shear rates (0.01, 0.1, 1, 10 and 100 s^{-1}) as a function of time at 22°C; b) Viscosity as a function of shear rate for both A2 and A3 formulations after 10 min at 22°C (mean; n≥3). The slope between 10 and 100 s-1 was used to evaluate the shear stress during printing using equation 1.

Recovery immediately after shear removal was only partial, especially for high shear rates, but curves show that viscosity continues to recover with time, and further increased when the temperature was increased to 37°C. For A2, the immediate recovery was much better for shear rate of 10 s-1 compared to 100 and 1000 s-1 (501 ± 127 Pa.s versus 66 ± 15 Pa.s and 2 ± 1 Pa.s respectively (see the complete data in Supplemental materials section Table S1). The difference was less drastic for A3 (10 and 100 s-1 curves are superposed, and viscosity at shear removal decreased from ~ 600 to 130 Pa.s depending on the shear rate value). Thus the viscosity values immediately after 100 s^{-1} shear removal was about 10 fold higher for A3 compared with A2 hydrogels (663 ± 95 Pa.s and 66 ±15 Pa.s, respectively).

Similar tests were performed on A3 solutions left for 20 min (instead of 10 min) at 22°C to mimic longer pre-printing times (Figure 4d). At these time points, even at 22°C, the solution has already begun to gel ($t \geq t_g$). However, no drastic impact was observed on recovery properties. Immediate recovery is slightly reduced, but viscosity then increases with time, reaching similar final values.

To confirm the importance of printing before gelation, we also performed recovery tests after 20 min gelation at 37°C. Results for A2 are presented in Figure 4(b), results for A3 in the supporting information (Figure S3). As expected, viscosity increased more during the rest period, due to hydrogel gelation at 37°C. Following shear, only partial immediate recovery was observed, without any further increase of the viscosity with time for A2 (Figure 4(b)), some increase for A3. The difference between A2 and A3 can be explained by the fact that A3 gelation is much slower than A2 gelation, as shown in Figure 2.

As a comparison, shear recovery tests were also performed on the control bioink consisting of 3%w/v alginate with 7% w/v gelatin [21] (Figure 5, and supplementary Table S2 for more complete data). Alginate/gelatin present a different behavior compared to chitosan hydrogels, with better immediate recovery of the viscosity, but no further increase with time. As for chitosan hydrogels, the extent of recovery decreased with increasing shear rates. Interestingly, the viscosity at rest, prior to shear, was found to increase with time. This could be explained by the change of temperature of the solution (which was poured in the rheometer at 25°C since it is too not liquid enough at 22°C due to the presence of gelatin). Another possible explanation is alginate-gelatin interactions after mixing the solution. In contrast, similar tests performed on pure alginate didn't show any variation of the viscosity at rest (data not shown).

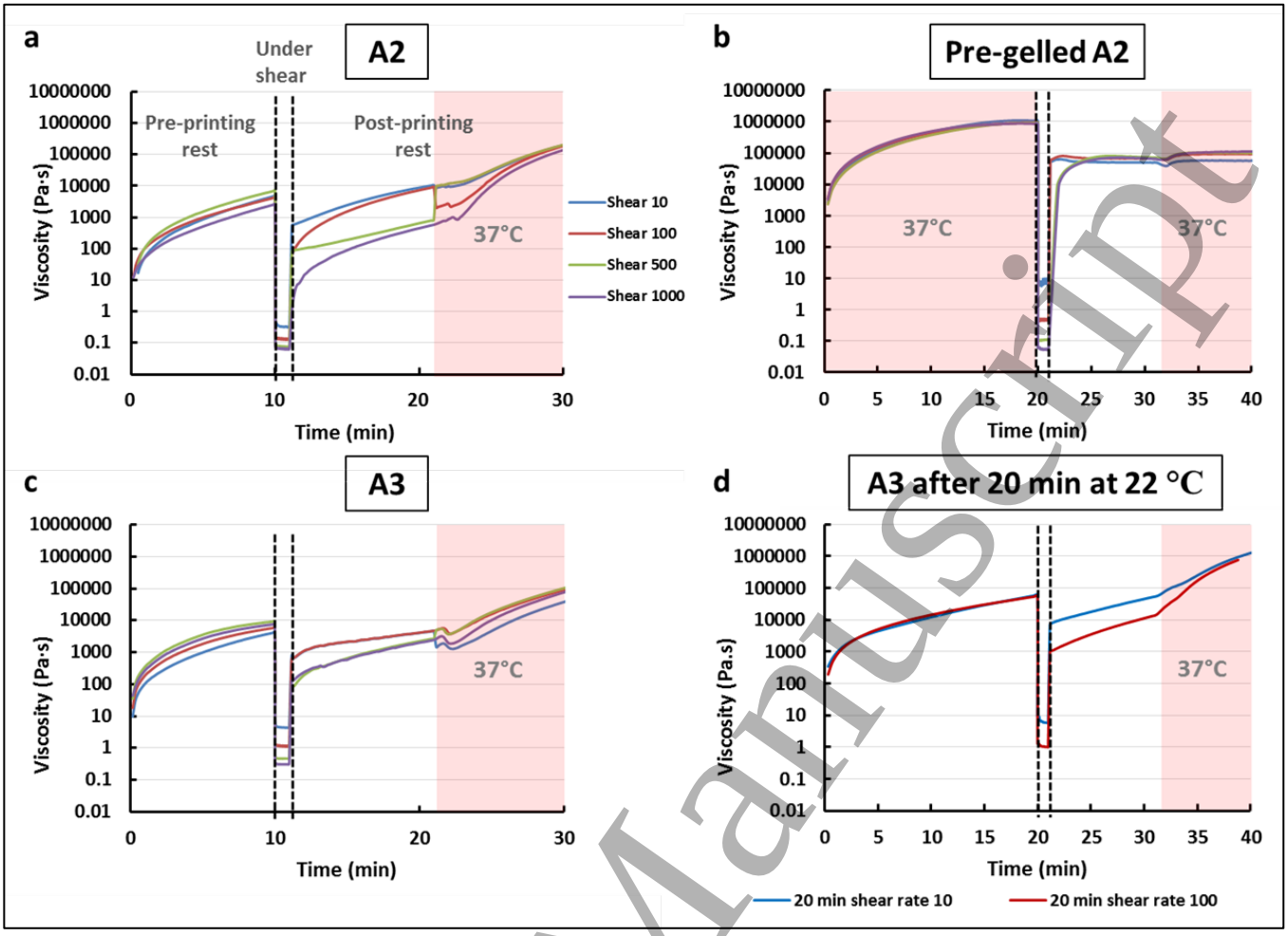

Figure 4. Shear viscosity recovery under 4 different applied shear rates (10, 100, 500, 1000 s^{-1}). The graphs present the complete cycle, namely at-rest state (shear at 0.001 s^{-1}, generally for 10 min), printing step (shear rate at one of the 4 different tested shear rates for 1 min), post printed rest state at 22°C and post-printed rest at 37°C (shear back at 0.001 s^{-1}): a) A2, b) Pre-gelled A2 (shear after gelation for 20 min at 37C); c)A3, d) A3 with 20min at rest instead of 10 min. The change of the shear rate is indicated with the vertical lines; Temperature 37°C is highlighted, otherwise 22°C) (mean +/-SD ; n≥3).

3.5 3D printing of pre-hydrogel solutions

To confirm the correlation between rheological data and printability in real printing conditions, the biomaterial inks were also printed using a 3D Discovery printer as described in the experimental section and in Table 2. The size of the needle (22G needle) and the flow rate (1.25 mm^3/min) were chosen in order to keep the shear rate applied on the gel during the extrusion close to 100 s^{-1}, according to equation 1. This value was chosen based on the results of the recovery tests, showing better recovery at such a low shear rate (Figure 4). The printing resolution was studied as a function of the feed rate (speed of needle above the substrate during deposition) and gel formulation. We analysed the width of the filaments after extrusion, the uniformity of the printed lines, their continuity and their integrity, which can be defined as the comparison of the theoretical and measured height of the printed filaments [22, 23].

B2 and B3 showed phase separation after centrifuge, even before printing (Figure S1(a)). Printing led to a heterogeneous mix of gel and liquid regions, with non-repeatable and broken filaments. In particular, B2 led to non-uniform filaments, broken lines and curvy angles (see the example in Figure S1(b)), which made it impossible to print multiple layer structures. Double phasing was even clearer for B3, leading to needle clogging and preventing good extrusion. Therefore, we do not present the complete data for B2 and B3 here.

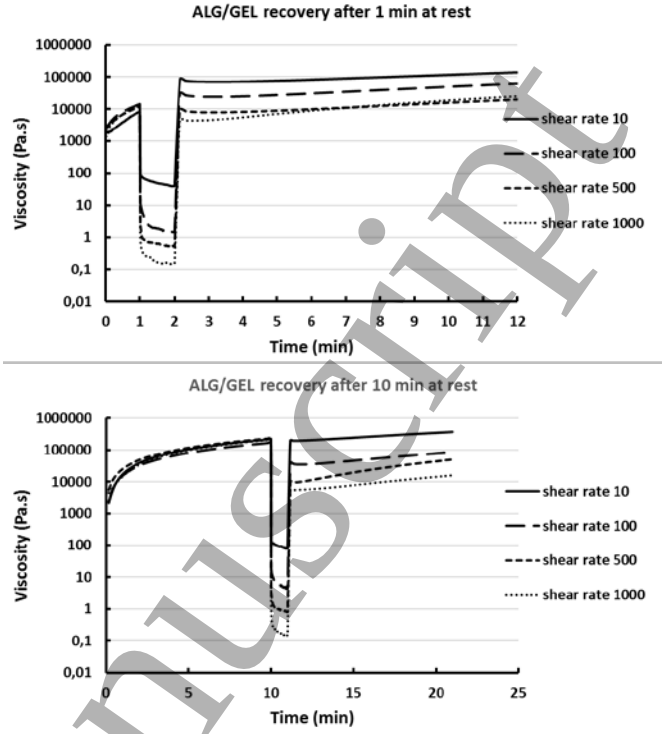

Figure 5. Shear recovery tests of Alginate/gelatin hydrogels after 1 or 10 min rest times (mimicking time in the cartridge before printing. Four different shear rates (10, 100, 500, 1000 s-1) were applied (mean; n=6).

Figure 6 presents data and typical images of printed lines for A2 and A3 formulations at various feed rates. Both formulations led to uniform filaments. As shown in Figure 6(a), A2 was able to print continuous lines with relatively sharp angles, but the filament width was large (1.2-1.5 mm) compared to the needle internal diameter (ratio of width/diameter = 3.5). This leads to low resolution.

A3 led to uniform, sharp angled and thinner filaments (minimum width of 0.57 mm ± 0.04 mm (ratio=1.4) at a feed rate of 11 mm/s (Figure 6b). However, at this feed rate, the lines were easily breaking, making it challenging to print multiple layer structures. Reducing the feed rate to 10 mm/s led to continuous lines with a mean width of 0.75 mm ± 0.07, making it a better option.

Printing multiple layer structures with A3 led to smooth integration between layers and cohesive structures (Fig 6(e)). To observe the structural integrity of the gel, we analysed the difference between the theoretical and the real height of 5- or 10-layer structures. The average height of the layers was found to be between 0.33 and 0.27 mm, which is a variation of ± 10% from the theoretical height (0.3 mm). This shows that the structure isn't collapsing under the weight of the multiple layers. The structure was also quite comparable to its theoretical CAD design (Fig 6(d)).

Interestingly, structures printed at higher shear rates (higher flow rates or similar flow rate but smaller needle diameter) led to poor resolution and structural integrity, as shown in Figure 7(a). This is in agreement with recovery tests which show better recovery at low shear rates.

Filament width with A3 was quite similar to that of alginate/gelatin (0.68 ±0.06 µm) which showed very uniform fiber formation (Figure 6 (b), (c)) and ability to print in a cohesive layer-by-layer structure before post-crosslinking (Figure 7a).

a

Bioink : A2
Gauge : 22G

Flow rate [mm^3/min]	Feed rate [mm/sec]	Continuity	Uniformity	Sharp Angle	Average width	std deviation
1.25	7	1	1	0	1.52	0.05
	8	1	1	0	1.40	0.17
	9	1	1	1	1.45	0.04
	10	1	0	1	1.23	0.28
	11	1	0	1	1.41	0.10

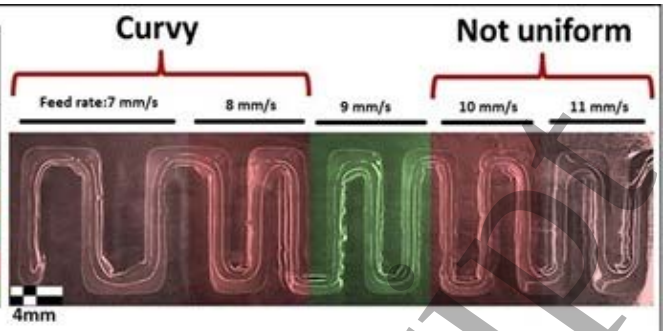

b

Bioink : A3
Gauge : 22G

Flow rate [mm^3/min]	Feed rate [mm/sec]	Continuity	Uniformity	Sharp Angle	Average width	std deviation
1.25	7	1	1	1	0.97	0.04
	8	1	1	1	0.99	0.05
	9	1	1	1	0.90	0.08
	10	1	1	1	0.75	0.07
	11	0	1	1	0.57	0.04

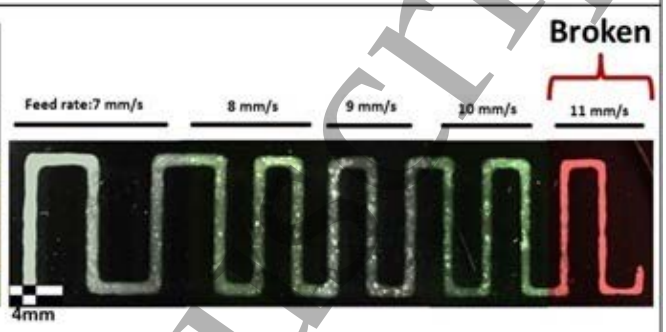

c

Bioink : Alg3Gel7
Gauge : 22G

Flow rate [mm^3/min]	Feed rate [mm/sec]	Continuity	Uniformity	Sharp Angle	Average width	std deviation
1.25	7	1	1	1	0.83	0.02
	8	1	1	1	0.74	0.06
	9	1	1	1	0.70	0.06
	10	1	1	1	0.68	0.06
	11	1	1	1	0.70	0.07

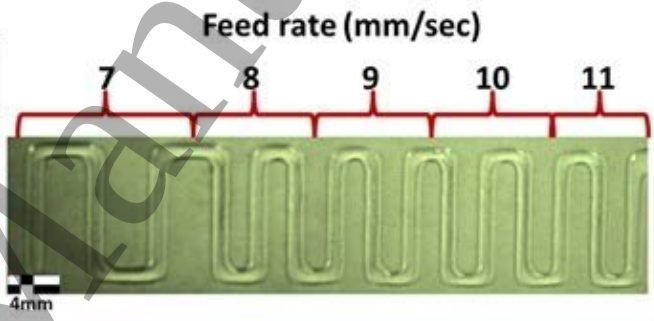

d

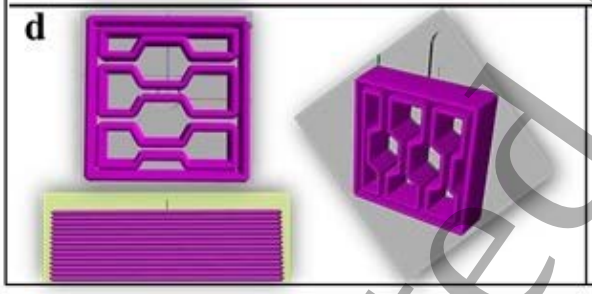

e

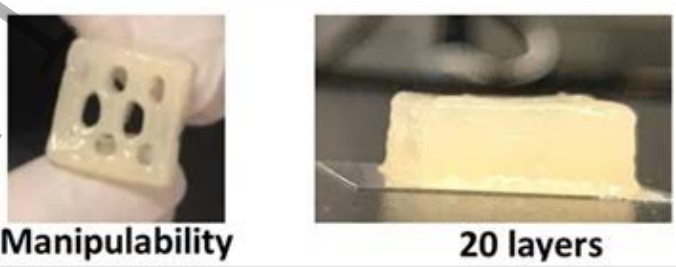

Figure 6. a) Descriptive results and images of filaments printed with a 22 G needle (0.41 mm inner diameter) with feed rates changing from 7 to 11 mm/s, for a) A2, b) A3 chitosan hydrogels and c) Alginate/gelatin filaments as comparison (mean +/- SD; n≥3).; d) 3D CAD honeycomb design model; e) picture of 10- and 20-layers printed structures made with A3 hydrogel.

3.6 Post printed mechanical strength

A good ink should provide tissue-mimicking rigidity and good mechanical strength after printing. The mechanical properties of printed structures were therefore tested in compression, after 24h gelation at 37°C (Figure 7). A3 formulation was chosen since it presented the best rheological properties in terms of adequate gelation kinetic and recovery, and printing behavior. Recovery tests suggested that A3 formulation presents better recovery when the shear rate stays at or below 100 s^{-1} (see Figure 4(c)). We hypothesized that the resolution and mechanical properties would thus be increased when printing the structure at low/medium shear rate (e.g. 230 s^{-1}, see Table 2) compared to high shear rate e.g. 507 s^{-1},

(generated by increasing the flow rate to 2.75 mm^3/s). Compression tests were performed on 5-layer structures since it is the best we could obtain when printing A3 at high flow rate.

Pictures, compression curves and secant Young moduli at 15 and 30% deformation are reported in Figure 7 for structures extruded at low and high shear, in comparison with structures printed with the alginate/gelatin bioink at 200 s^{-1} (flow rate of 1.25 $mm^3.s^{-1}$), soaked in $CaCl_2$ for 15 min to ensure that the structure is completely crosslinked, then incubated at 37°C for 24 hours [25].

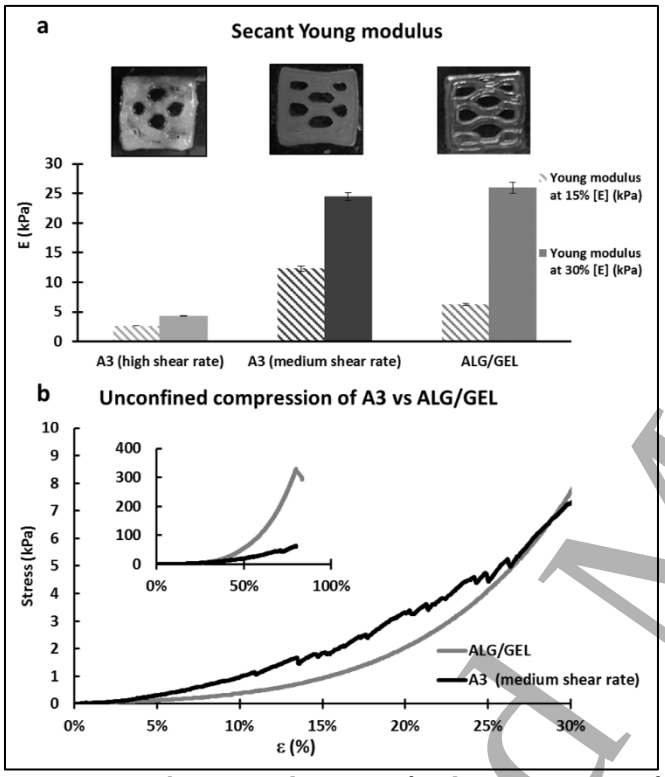

Figure 7. Behavior under unconfined compression of chitosan-based hydrogel and Alginate/Gelatin: a) secant Young modulus of A3 printed with high (507 s^{-1})/medium (230 s^{-1}) shear rate and alginate/gelatin bioinks; pictures of the 5-layer honeycomb structures tested are also shown; b) stress-strain curve in unconfined compression (mean ± SD; n≥3).

When printed at a low/medium shear rate (230 s-1), the secant Young modulus of A3 chitosan structures at 15 and 30% deformation was 12.3 ± 0.5 kPa and 24.4 ± 0.7 kPa respectively. This is similar to or even more rigid than alginate/gelatin bioink (6.3± 0.2 kPa and 25.9 ± 0.9 kPa at 15% and 30% deformation respectively). Both structures presented good integrity and were easily handable, even if alginate/gelatin structures presented significantly higher resistance to rupture (329 ± 27 kPa vs 48 ± 4 kPa for A3; Figure 7b).

As expected, the mechanical properties of A3 chitosan gel printed at high shear rate (e.g. 507 s^{-1}) were lower. The secant Young modulus at 15% and 30% deformation was 2.6 ± 0.02 kPa and 4.3± 0.1 kPa, respectively. The printed structure had a poor resolution. It was flattened and its poor structural integrity prevent it from being removed from the glass slide after printing.

4. Discussion

Inks for bioprinting must fulfil a number of key requirements, including printability and mechanical cohesion after printing [17]. Chitosan thermosensitive hydrogels formed with BGP, alone or combined with gelatin or hydroxyapatite have be previously shown to present interesting characteristics for bioprinting [15, 26] but they face particular challenges since they are time- and temperature-evolving materials.

While CH is normally soluble only in acidic media, the addition of a weak base such as BGP allow to form a solution with neutral pH at room temperature. The negatively charged molecules screen the chitosan positively charged ammonium groups and prevents repulsive forces between chitosan chains. When increasing temperature, heat-induced transfer of protons from CH to glycerol phosphate takes place, allowing strong interaction of CH chains, mainly through hydrophobic and hydrogen bonds [27, 28]. In the case of SHC+BGP or SC+PB, the higher mechanical properties observed could be explained by a more complete neutralization of chitosan chains due to the small size of SHC molecule and stronger interactions due to its decomposition into CO_2 [29]. While this physical gelation mainly takes place at temperature close to body temperature (due to the change of chitosan pKa), it initiates at lower temperatures. Some ionic crosslinking can also take place [28]. The lack of complete stability of the solution at room temperature is a possible limitation of these gels for bioprinting applications and must be taken into account by a rigorous rheological approach.

Yet to date, only limited rheological characterization has been performed [14, 15], which doesn't take time into account and doesn't allow to understand the benefits and limitations and optimize the printing process. In this work, we adapted rheological tests to assess and predict the printability of chitosan thermosensitive hydrogels, whose rheological properties evolve with temperature but also with time.

Gelation kinetics: We first performed time sweeps at 22°C to compare the various gel formulations in terms of stability at room temperature, i.e. how fast does the gelation start when the solution is kept in a cartridge at room temperature. This information is important since the time required to prepare the set-up and print can change the bioink properties. Crosslinking of the solution prior to extrusion could lead to needle clogging [19, 30] or to decreased shear thinning or poor recovery after shear removal.

Formulations made with a mixture of SHC+BGP (A) presented better stability at room temperature than their SHC+PB (B) counterparts, the latter presenting a gelation time of less than 30 s according to the approach of Winter and Chambon. This is in accordance with our previous data [11]. It is however important to mention that this approach (assessing gelation time by G' and G'' crossover) has limitations.

The fast gelation of SHC-PB formulations (especially B3) at room temperature can be correlated with the precipitation and phase separation observed during the centrifugation process prior to cartridge loading, as well as to the heterogeneous and non-continuous structures at printing (Figure S1) at even room temperature. These formulations were therefore rapidly discarded.

Time sweeps at 37°C allowed us to evaluate the ability of the material to rapidly gel at 37°C. One advantage of thermosensitive hydrogels for bioprinting is the increase of their mechanical properties once incubated at 37°C, without the need of a crosslinker. Results confirmed that increasing the temperature to 37°C accelerates the gelation process in all chitosan-based bioinks, but the effect was more pronounced for CH2%w/v formulations (A2). The lower thermosensitivity of CH3% compared to CH2% hydrogel is in accordance with literature data [31, 32] and could be explained by decreased diffusion of bicarbonate molecules (SHC) and reduced movement of chitosan chains, leading to less chain interactions.

The more pronounced thermosensitivity of CH2% formulations could be an advantage for bioprinting. However, CH2% formulations also present lower viscosity before and after shear removal, which was later shown to be a more decisive property.

Shear thinning: In addition to adequate gelation time, shear-thinning behavior, characterized by viscosity decrease when the shear rate increases, is advantageous for bioprinting. This property makes it possible to reduce the pressure needed to extrude the material and therefore the potential damage to the cells encapsulated in the hydrogel via plug flow behavior [33-35]. More shear-thinning hydrogels present fewer cell damages during extrusion. Our results showed that all pre-hydrogel solutions tested were non-Newtonian, and presented shear thinning behavior (Figure 3). At a shear rate of 100 s^{-1}, the dynamic viscosity of A3 formulation was about 10^3 mPa.s, which corresponds to shear stresses of 100 Pa.

Alginate-gelatin control hydrogels also presented shear thinning properties but to a lower extent (viscosity around 10^5 mPa.s at 100 s^{-1}; Figure S2). It suggests that applied shear stress will be 10000 Pa on cells at e.g. shear rate of 100 s^{-1}. Impact of shear stress on cell viability was studied by other researchers [34, 35]. It was reported that shear stress above 5000 Pa influences cell survival adversely in both the short- and long term [34, 35]. However, further studies are required to prove chitosan hydrogel's advantages over alginate/gelatin as bioink for cell encapsulation.

The information extracted from the shear viscosity results can assist in gaining a better understanding of a biomaterial ink or bioink's extrudability in printing. Moreover, its slope allows to evaluate the shear stress during printing as a function of flow rate and needle diameter. This approach can be applied to any extrusion-based system. However, printability cannot be concluded from these results alone [17, 36]. Shear recovery was therefore performed as a next test.

Shear recovery and printability: Since shear during printing can alter the material's properties, it is important to verify that the biomaterial ink rapidly recovers after shear, to maintain the printed structure. Therefore, shear recovery tests were performed on formulations made with SHC+BGP (A2, A3). An additional step was added to common recovery tests, i.e. temperature increase at 37°C to mimic sample heating after printing to take advantage of the gel thermosensitive properties.

Data showed that the ability to recover after shear depends on the formulation (A3 better than A2), the extent of shear rate (better recovery for shear rate of 100 s^{-1} or less), and the extent of gelification of the hydrogel prior to shear. As expected, shear recovery was very limited for the pre-gelled inks. These results show the importance of the stability of the solution at room temperature, when the solution is in the printing cartridge, and to control the time during which the solution is kept in the cartridge before printing. Change of viscosity and beginning of gelation is a limitation of chitosan thermogels compared to other bioinks. We therefore suggest to control the flow rate using a plunger dispenser in contrast to pressure-

driven extrusion, as we did in our study, to avoid flow variability during printing. However, recovery after printing can still vary as a function of time between hydrogel mixing and printing. It is therefore important to evaluate the acceptable time frame for extrusion.

Chitosan 3% (A3) presented better recovery compared to chitosan 2% formulation (A2), especially at low and medium shear rates. This suggests that A3 filaments present a better ability to support upper layers, as it was indeed observed later during printability tests. Indeed, A3 presented lower filament width, and a better conformity of the printed structure to the CAD design. The resolution could be further enhanced by finding a bioink formulation showing fast and complete recovery after shear removal, as was observed for alginate/gelatin ink (Figure 5 and 6 (c)).

It is also important to note that in the case of A2, the filament width was significantly larger than for A3, the filament width/needle diameter ratio reaching up to 3.5, compared to 1.4 (Figure 6 (a) & (b)). This indicates that the gel is taken expansion after extrusion, and could be related to the normal force that impact extruded filament during extrusion process [37].

These two reasons could explain the difficulty of bioprinting solid 3D structures with A2 hydrogels, despite their more interesting thermosensitive character.

In contrast, A3 presented high initial viscosity, good shear thinning and good recovery when printed at a low shear rate, leading to 3D structures with good integrity and a rigidity comparable to alginate/gelatin at the low deformation rate generally encountered in biological tissues (<30%). Variation between the theoretical and real height of the printed structure was less than 10% and the printed structure was close to the CAD model (Figure 6(d), (e)). This shows that there is no significant spreading of the printed filaments and that they support the weight of the additional layers. Moreover, the printed structure showed excellent cohesion between layers and was easy to handle This is an important result since mechanical properties are key to ensure the fidelity of the structure during printing, but also later to ensure cohesion during maturation, handling and potential in vivo stresses. It also influence cell response [33, 38].

Recovery tests however emphasize the importance of the shear rate during printing. Indeed, recovery was poorer after high shear rates. Inability to return to the reference viscosity implies loss of chain interactions in the physical hydrogel. This was reflected by the appearance and the mechanical properties of the printed structures, which were much poorer for the 3D structure printed at a shear rate of 507 s^{-1} than at 230 s^{-1} (Figure 7(a)). Evaluating the shear stress using shear thinning tests and equation 1, and performing recovery test at the corresponding shear stress would therefore be an important step to assess the printability or optimize the printing process of biomaterial inks.

The cytocompatibility of chitosan-based hydrogels for cell encapsulation has been already proven, by our team among others [11, 12, 14, 39, 40]. But for their use as bioinks, further work is of course needed to study the influence of gel formulation and shear rates on the survival of encapsulated cells. Further optimization could also be performed by the addition of gelatin or collagen, which have been shown to improve cell adhesion, survival and migration and could also influence [14, 39-41] and improve their printability.

Another limitation of this work is that while the substrate was heated at 37°C, temperature can be lower on top layers. Further work will be required to better assess the effect of the substrate's temperature and possible variability of the temperature among the various layers to determine the importance of a well-controlled print bed to create homogenous structures. However, it is important to mention that we didn't observe heterogeneity in the structures created by 10 or 20 layers after 24 hour gelation in an incubator.

Another potential limitation with chitosan as a bioink is that, as all biopolymers, it presents high batch to batch variability. This is why we couldn't reproduce exactly the same rheological properties and had to change the concentration of gelling agent, compared to our previous publication [11, 42]. Characterization of chitosan molecular weight and deacetylation degree to select the right batch is therefore is important to decrease this variability. Moreover, the variability of the results must be determined using sufficient sample number and independent repetitions of each test.

As expected, alginate/gelatin hydrogels presented interesting recovery properties, despite also dependant of the shear rate. Such behavior is similar than for pure alginate bioink, according to the literature data [19, 43]. In this study, alginate/gelatin was studied as considered as a stable solution since we kept the temperature constant at 22°C. We however noted that the viscosity at rest increased with time. This is probably due to the slight decrease of the temperature between the moment the material was poured in the rheometer (at 25°C) and the time it stabilizes at 22°C. Indeed, the viscosity of gelatin is strongly dependant on the temperature. It might also be due to interactions between alginate and gelatin after

mixing. This emphasizes the importance of evaluating the effect of time and temperature during printability studies. Thus, the present approach could be applied to other temperature or time-evolving materials.

5. Conclusion

In this work, we propose a rheological approach to evaluate the printability of biomaterials inks, in particular for the case of time- and temperature-evolving materials such as chitosan thermosensitive hydrogels. The method to calculate the shear stress can be universally applied for any type of extrusion-based system. We showed that gelation kinetic, shear thinning and shear recovery tests where time and temperature is taken into account, are essential to evaluate the printability of time-evolving bioinks.

The gelation kinetics and the level of shear rate had a critical effect on shear recovery. It strongly influenced the ability to support layer-by-layer build-up, the fidelity of the printed structure and its post-printing mechanical properties.

One formulation made with sodium bicarbonate and beta-glycerophosphate as gelling agent (A3) appears a promising bioink. After 24 hours gelation at 37°C, it presents similar rigidity in compression at the low deformation (<30%, generally encountered in biological tissues) than alginate/gelatin bioink after crosslinking by calcium ions. However, its mechanical resistance is lower. Its biodegradability is a clear advantage over alginate-based bioinks which degradation is depending of many parameters and is difficult to control [44]. However, further work is needed to confirm cell viability and proliferation in these new chitosan-based bioinks.

Acknowledgement

We would like to acknowledge the Natural Science and Engineering Research Council of Canada (NSERC; RGPIN-2015-05169) and the Fonds de Recherche du Quebec – Nature et technologie (FRQNT; team project and M.R. scholarship) for funding and support of this project.

References

1. Groll, J., et al., *A definition of bioinks and their distinction from biomaterial inks.* Biofabrication, 2018. **11**(1): p. 013001.
2. Jones, T.D., *Extrusion Based Bioprinting: An In Vitro Model for Dental Pulp Tissue Engineering*. 2018.
3. Hsu, L. and X. Jiang, *'Living'Inks for 3D Bioprinting.* Trends in biotechnology, 2019.
4. Panwar, A. and L.P. Tan, *Current status of bioinks for micro-extrusion-based 3D bioprinting.* Molecules, 2016. **21**(6): p. 685.
5. Chimene, D., et al., *Advanced bioinks for 3D printing: a materials science perspective.* Annals of biomedical engineering, 2016. **44**(6): p. 2090-2102.
6. Gao, T., et al., *Optimization of gelatin–alginate composite bioink printability using rheological parameters: A systematic approach.* Biofabrication, 2018. **10**(3): p. 034106.
7. Seol, Y.-J., et al., *Bioprinting technology and its applications.* European Journal of Cardio-Thoracic Surgery, 2014: p. ezu148.
8. Chenite, A., et al., *Rheological characterisation of thermogelling chitosan/glycerol-phosphate solutions.* Carbohydrate polymers, 2001. **46**(1): p. 39-47.
9. Yao, M., et al., *Chitosan-based thermosensitive composite hydrogel enhances the therapeutic efficacy of human umbilical cord MSC in TBI rat model.* Materials Today Chemistry, 2019. **14**: p. 100192.
10. Xu, H., et al., *Enhanced cutaneous wound healing by functional injectable thermo-sensitive chitosan-based hydrogel encapsulated human umbilical cord-mesenchymal stem cells.* International journal of biological macromolecules, 2019. **137**: p. 433-441.
11. Assaad, E., M. Maire, and S. Lerouge, *Injectable thermosensitive chitosan hydrogels with controlled gelation kinetics and enhanced mechanical resistance.* Carbohydrate polymers, 2015. **130**: p. 87-96.
12. Ceccaldi, C., et al., *Optimization of injectable thermosensitive scaffolds with enhanced mechanical properties for cell therapy.* Macromolecular bioscience, 2017. **17**(6).
13. Monette, A., et al., *Chitosan thermogels for local expansion and delivery of tumor-specific T lymphocytes towards enhanced cancer immunotherapies.* Biomaterials, 2016. **75**: p. 237-249.
14. Roehm, K.D. and S.V. Madihally, *Bioprinted chitosan-gelatin thermosensitive hydrogels using an inexpensive 3D printer.* Biofabrication, 2017. **10**(1): p. 015002.
15. Demirtaş, T.T., G. Irmak, and M. Gümüşderelioğlu, *A bioprintable form of chitosan hydrogel for bone tissue engineering.* Biofabrication, 2017. **9**(3): p. 035003.
16. Dealy, J. and K. Wissbrun, *Melt rheology and its role in plastics processing: Theory and applications*. 1990, New York, Van Nostrand Reinhold.
17. Hölzl, K., et al., *Bioink properties before, during and after 3D bioprinting.* Biofabrication, 2016. **8**(3): p. 032002.
18. Kesti, M., et al., *Guidelines for standardization of bioprinting: a systematic study of process*

parameters and their effect on bioprinted structures. BioNanoMaterials, 2016. **17**(3-4): p. 193-204.

19. Paxton, N., et al., *Proposal to assess printability of bioinks for extrusion-based bioprinting and evaluation of rheological properties governing bioprintability.* Biofabrication, 2017. **9**(4): p. 044107.
20. Guvendiren, M., H.D. Lu, and J.A. Burdick, *Shear-thinning hydrogels for biomedical applications.* Soft matter, 2012. **8**(2): p. 260-272.
21. Jiang, T., et al., *Directing the self-assembly of tumour spheroids by bioprinting cellular heterogeneous models within alginate/gelatin hydrogels.* Scientific reports, 2017. **7**(1): p. 4575.
22. Gillispie, G., et al., *Assessment methodologies for extrusion-based bioink printability.* Biofabrication, 2020. **12**(2): p. 022003.
23. Webb, B. and B.J. Doyle, *Parameter optimization for 3D bioprinting of hydrogels.* Bioprinting, 2017. **8**: p. 8-12.
24. Winter, H.H. and F. Chambon, *Analysis of linear viscoelasticity of a crosslinking polymer at the gel point.* Journal of rheology, 1986. **30**(2): p. 367-382.
25. Chung, J.H., et al., *Bio-ink properties and printability for extrusion printing living cells.* Biomaterials Science, 2013. **1**(7): p. 763-773.
26. Tonda-Turo, C., et al., *Photocurable chitosan as bioink for cellularized therapies towards personalized scaffold architecture.* Bioprinting, 2020. **18**: p. e00082.
27. Lavertu, M., D. Filion, and M.D. Buschmann, *Heat-induced transfer of protons from chitosan to glycerol phosphate produces chitosan precipitation and gelation.* Biomacromolecules, 2008. **9**(2): p. 640-650.
28. Cho, J., et al., *Physical gelation of chitosan in the presence of β-glycerophosphate: the effect of temperature.* Biomacromolecules, 2005. **6**(6): p. 3267-3275.
29. Alinejad, Y., et al., *An injectable chitosan/chondroitin sulfate hydrogel with tunable mechanical properties for cell therapy/tissue engineering.* International journal of biological macromolecules, 2018. **113**: p. 132-141.
30. Ouyang, L., et al., *Effect of bioink properties on printability and cell viability for 3D bioplotting of embryonic stem cells.* Biofabrication, 2016. **8**(3): p. 035020.
31. Cho, J., et al., *Chitosan and glycerophosphate concentration dependence of solution behaviour and gel point using small amplitude oscillatory rheometry.* Food Hydrocolloids, 2006. **20**(6): p. 936-945.
32. Zhou, H.Y., et al., *Glycerophosphate-based chitosan thermosensitive hydrogels and their biomedical applications.* Carbohydrate polymers, 2015. **117**: p. 524-536.
33. Aguado, B.A., et al., *Improving viability of stem cells during syringe needle flow through the design of hydrogel cell carriers.* Tissue Engineering Part A, 2011. **18**(7-8): p. 806-815.
34. Blaeser, A., et al., *Controlling shear stress in 3D bioprinting is a key factor to balance printing resolution and stem cell integrity.* Advanced healthcare materials, 2016. **5**(3): p. 326-333.
35. Foster, A.A., L.M. Marquardt, and S.C. Heilshorn, *The diverse roles of hydrogel mechanics in injectable stem cell transplantation.* Current opinion in chemical engineering, 2017. **15**: p. 15-23.
36. Murphy, S.V. and A. Atala, *3D bioprinting of tissues and organs.* Nature biotechnology, 2014. **32**(8): p. 773.
37. Dealy, J.M. and K.F. Wissbrun, *Melt rheology and its role in plastics processing: theory and applications.* 2012: Springer Science & Business Media.
38. Dubbin, K., A. Tabet, and S.C. Heilshorn, *Quantitative criteria to benchmark new and existing bio-inks for cell compatibility.* Biofabrication, 2017. **9**(4): p. 044102.
39. Cheng, N.-C., et al., *Sustained release of adipose-derived stem cells by thermosensitive chitosan/gelatin hydrogel for therapeutic angiogenesis.* Acta biomaterialia, 2017. **51**: p. 258-267.
40. Tang, Q., et al., *Thermosensitive chitosan-based hydrogels releasing stromal cell derived factor-1 alpha recruit MSC for corneal epithelium regeneration.* Acta biomaterialia, 2017. **61**: p. 101-113.
41. Dang, Q., et al., *Fabrication and evaluation of thermosensitive chitosan/collagen/α, β-glycerophosphate hydrogels for tissue regeneration.* Carbohydrate polymers, 2017. **167**: p. 145-157.
42. Ceccaldi, C., et al., *Optimization of Injectable Thermosensitive Scaffolds with Enhanced Mechanical Properties for Cell Therapy.* Macromolecular Bioscience, 2017.
43. Li, H., S. Liu, and L. Lin, *Rheological study on 3D printability of alginate hydrogel and effect of graphene oxide.* Int J Bioprinting, 2016. **2**(2): p. 54-66.
44. Asti, A. and L. Gioglio, *Natural and synthetic biodegradable polymers: different scaffolds for cell expansion and tissue formation.* The International journal of artificial organs, 2014. **37**(3): p. 187-205.

Figure captions

Figure 1. Schematic of the applied shear rates and temperature as a function of time during recovery tests.

Figure 2. Gelation kinetics of A and B chitosan-based hydrogels: a) Evolution of the storage (G') and loss (G'') moduli of hydrogels as a function of time at 22°C (mean +/-SD; n≥3). b) Evolution of the storage (G') and loss (G'') moduli as a function of time at 37°C. c) G' value after 10 min at 22°C and 1h at 37°C, respectively (mean +/-SD; n≥3); (** p<0.01, *** p<0.001, **** p<0.0001). Gels were made with SHC+BGP as gelling agents, while B gels were prepared with SHC+PB, as described in Table 1.

Figure 3. Shear thinning behavior of: a) viscosity of A3 formulations at various shear rates (0.01, 0.1, 1, 10 and 100 s^{-1}) as a function of time at 22°C; b) Viscosity as a function of shear rate for both A2 and A3 formulations after 10 min at 22°C (mean; n≥3). The slope between 10 and 100 s-1 was used to evaluate the shear stress during printing using equation 1.

Figure 4. Shear viscosity recovery under 4 different applied shear rates (10, 100, 500, 1000 s^{-1}). The graphs present the complete cycle, namely at-rest state (shear at 0.001 s^{-1}, generally for 10 min), printing step (shear rate at one of the 4 different tested shear rates for 1 min), post printed rest state at 22°C and post-printed rest at 37°C (shear back at 0.001 s^{-1}): a) A2, b) Pre-gelled A2 (shear after gelation for 20 min at 37C); c)A3, d) A3 with 20min at rest instead of 10 min. The change of the shear rate is indicated with the vertical lines; Temperature 37°C is highlighted, otherwise 22°C) (mean +/-SD; n≥3).

Figure 5. Shear recovery tests of Alginate/gelatin hydrogels after 1 or 10 min rest times (mimicking time in the cartridge before printing. Four different shear rates (10, 100, 500, 1000 s-1) were applied (mean; n=6).

Figure 6. a) Descriptive results and images of filaments printed with a 22 G needle (0.41 mm inner diameter) with feed rates changing from 7 to 11 mm/s, for a) A2, b) A3 chitosan hydrogels and c) Alginate/gelatin filaments as comparison (mean +/-SD; n≥3).; d) 3D CAD honeycomb design model ; e) picture of 10- and 20-layers printed structures made with A3 hydrogel.

Figure 7. Behavior under unconfined compression of chitosan-based hydrogel and Alginate/Gelatin: a) secant Young modulus of A3 printed with high (507 s^{-1})/medium (230 s^{-1}) shear rate and alginate/gelatin bioinks; pictures of the 5-layer honeycomb structures tested are also shown; b) stress-strain curve in unconfined compression (mean ± SD; n≥3).

Table captions

Table 1. Concentration of chitosan and gelling agents of the various tested hydrogels (CH: Chitosan, BGP: Beta-glycerophosphate, SHC: Sodium hydrogen carbonate, PB: Phosphate buffer at pH=8).

Table 2. Printing parameters used on the 3D Discovery bioprinter: needle size, n-1 slope according to viscosity vs shear rate graph and corresponding shear rate as a function of needle size according to equation 1. Constant parameters were: Flow rate = 1.25 µL/s (mm^3/s); feed rate = 6 mm/s; layer thickness = 0.3 mm.